Front. Phys. 13(2), 137501 (2018)
https://doi.org/10.1007/s11467-017-0722-6

RESEARCH ARTICLE

AC-current-induced magnetization switching in amorphous microwires

V. Zhukova[1,2], J. M. Blanco[2], A. Chizhik[1,2], M. Ipatov[2], A. Zhukov[1,2,3,†]

[1] *Dpto. Física Aplicada I, EUPDS, UPV/EHU, Plaza Europa 1, San Sebastián, 20018, Spain*
[2] *Dpto. Física de Materiales, Facultad de Química, UPV/EHU, 1072, 20080, San Sebastián, Spain, and*
[3] *IKERBASQUE, Basque Foundation for Science, 48011 Bilbao, Spain*
Corresponding author. E-mail: [†] *arkadi.joukov@ehu.es*
Received February 15, 2017; accepted June 20, 2017

We studied the influence of AC current flowing through microwires, on magnetization dynamics. We used a previously developed Sixtus-Tonks modified setup to evaluate the domain wall (DW) velocity within the microwire. However, instead of a magnetizing solenoid, we used a current flowing through the microwire. We observed that the AC current flowing through the annealed Co-rich microwire leads to remagnetization by fast domain wall propagation. The estimated DW velocity was approximately 4.5 km/s, which is similar to and even higher than that reported for the magnetic-field-driven domain wall propagation in Fe- and Co-rich microwires. We measured the DW velocity under tensile stress, and found that the DW velocity decreases under applied stress. An observed DW propagation induced by the current flowing through the microwire is explained considering the influence of an Oersted magnetic field on the outer domain shell. This field has a circular easy magnetization direction and magnetostatic interaction between the outer circumferentially magnetized shell and the inner axially magnetized core.

Keywords domain wall propagation, magnetic microwire, amorphous material, magnetoelastic anisotropy

PACS numbers 75.60.Ej, 75.60.Jk

1 Introduction

The engineering of domain wall (DW) dynamics in nano- and microwires is a challenge for fundamental physics and technological applications related to magnetic recording and magnetic sensors [1, 2]. In these applications, the DW serves as the logic gate or memory element.

The magnetic-field-driven domain wall propagation in different families of magnetic wires is a conventional topic of research. The most basic phenomena of domain wall dynamics, such as the existence of a domain wall nucleation and the concept of domain wall mobility, were established in previous works [3–5]. Moreover, applications of domain wall dynamics to magnetic bubble memories, in which information is stored in small magnetized areas delimited by domain walls and written by displacement of the walls under magnetic fields, were proposed more than 30 years ago [4].

Several years ago, an alternative approach to using current-induced magnetic domain wall propagation in magnetic wires was proposed [1, 2, 6]. Consequently, control of the domain wall motion induced by a magnetic field and/or by a current flowing directly into the magnetic element is a recent issue in magnetism as well as a technological challenge. Additionally, the DW velocity value is critical in the aforementioned applications.

On the other hand, electric-current-driven and magnetic-field-driven DW dynamics present rather different features. Current-induced DW propagation has considerably different features from magnetic-field-driven propagation, making the former particularly useful for memory storage applications [6]. When using a current-induced DW movement, each DW moves in the same direction, maintaining the overall magnetic structure in the wire [6]. For thin magnetic wires (typically permalloy, $Ni_{81}Fe_{19}$), a current-driven DW motion occurs if the current density exceeds a threshold value on the order of 10^8 A/cm^2. Such elevated current densities

are impractical for device applications, and it is crucial to find methods to reduce this threshold value. Moreover, for amorphous magnetic microwires, these current densities can be critical owing to Joule heating: the magnetic softness typical of amorphous magnetic wires can be destroyed [7]. Direct and indirect experiments indicate that for amorphous microwires, there is considerable Joule heating at current densities above 470 A/mm^2, and even short current pulses considerably affect the magnetic properties [7, 8]. Therefore, Joule heating must be carefully avoided in order to maintain the soft magnetic character of amorphous microwires.

The Oersted magnetic field produced by current pulses can play an important role, considering the high current density involved [9]. Thus, for a current of 2×10^{12} A/m^2, a transverse field close to 8 kA/m can be produced [9]. In any case, for nanowires, it is demonstrated that the aforementioned Oersted field does not considerably affect the domain wall velocity [9]. The case of Co-rich amorphous magnetic microwires is completely different: using transverse magnetooptical Kerr effect (MOKE) magnetometry, we observed that the electrical current flowing through a magnetically soft Co-rich microwire can give rise to the remagnetization of the domains on the surface of the microwires [10]. This considerable difference can be attributed to the much softer magnetic properties of Co-rich microwires as compared to FeNi nanowires. Moreover, it is commonly assumed and experimentally confirmed that Co-rich microwires present a circular magnetization orientation of the outer domain shell [10–13]. Therefore, circular magnetic field created by electrical current can produce magnetization process in the surface domains of Co-rich microwires.

On the other hand, amorphous microwires with positive magnetostriction coefficient microwires present a magnetically bistable character: under the application of a longitudinal magnetic field opposite to the remanent magnetization, a large Barkhausen jump occurs [14–18]. The magnetization reversal of these microwires runs through a fast domain wall (DW) propagation [14–17].

A DW speed above 1000 m/s was reported for amorphous magnetic microwires [14–16], although less attention has been paid to the manipulation of DW dynamics [16, 17]. Thus, recently, DW braking and even trapping at a given position under the effect of an additional antiparallel local magnetic field were reported. That position and the DW velocity are further controlled by suitable tuning of the local field. Low parallel-local field generated tail-to-tail and head-to-head pairs of walls move along opposite directions when that field is strong enough [14, 17]. On the other hand, when manipulating the magnetoelastic energy through the application of tensile stress, changes to the magnetostriction constant and the internal stresses significantly affect the DW dynamics in magnetically bistable microwires [16].

The origin of the aforementioned spontaneous magnetic bistability in Fe-rich microwires is related to the peculiar domain structure of these microwires consisting of a single axial domain surrounded by a radial domain structure [12, 13].

Recently, we reported that in Co-rich microwires with low and negative magnetostriction coefficient present linear hysteresis loop in the as-prepared state and a magnetic bistability can be induced by thermal treatment [19, 20].

The main interest in Co-rich microwires with low magnetostriction coefficient is related to the giant magneto-impedance (GMI) effect. This GMI effect consists of a large change in the electrical impedance in a magnetic conductor subjected to an axial *dc* magnetic field H [21–23]. The GMI effect originates from the dependence of the transverse magnetic permeability upon the *dc* magnetic field and skin effect.

The aforementioned GMI effect is a promising phenomenon, exhibiting the highest sensitivity to magnetic fields among cryogen-free technologies, and is therefore suitable for designing various magnetic sensors and magnetometers with a pico-Tesla resolution achieved at room temperature [21–24].

Recently, we reported that Co-rich microwires with induced magnetic bistability can present elevated GMI effects and fast domain wall propagation in the same sample. These are features that were previously reported for completely different families of magnetic microwires [19, 20].

The elevated GMI effect observed in annealed Co-rich microwires with a rectangular hysteresis loop has been attributed to the circular magnetization orientation of the outer domain shell [19, 20]. On the other hand, the fast domain wall propagation of a single-domain wall has been attributed to the magnetization switching within the inner axially magnetized core with an axial magnetization orientation [19, 20].

Recently, we studied the magneto-impedance (MI) effect of amorphous Co-rich microwires at MHz and GHz frequencies, and observed the GMI hysteresis originating from the magnetostatic interaction of the inner axially magnetized core with the outer domain shell [25].

The rather different magnetic properties of microwires with positive and negative magnetostriction coefficients are related to their different domain structures. The outer domain shell of Fe-rich microwires presents a radial magnetization direction, while for Co-rich microwires, a circumferential magnetization orientation is reported elsewhere [19, 20, 26].

This difference can give rise to considerably different magnetization mechanisms. As mentioned above, using

MOKE, we observed that the electrical current flowing through the Co-rich microwire with a circular magnetization orientation in the outer domain shell can give rise to the remagnetization of the domains on the surface of the microwires [10]. On the other hand, it has not yet been studied if the remagnetization of the outer circular domains induced by electrical current affects the magnetization of the inner axially magnetized domain in Co-rich microwires with induced magnetic bistability. It is not clear if the remagnetization of the outer circular domains induced by electrical current runs through the single-domain wall propagation or multiple domain wall nucleation and growth.

Considering our recent results on the magnetostatic interaction of the inner axially magnetized core with the outer domain shell observed in as-prepared Co-rich microwires with linear hysteresis loops, we can assume that the existence of the magnetostatic interactions between the inner core and outer shell of Co-rich microwires with induced magnetic bistability present both a GMI effect and induced magnetic bistability. Therefore, similar to the influence of the inner axially magnetized core on the GMI effect, we expect that the changes induced in the outer domain shell can affect the magnetization in the inner core.

In this paper, we present the results of a successful attempt to manipulate the magnetization switching in the inner core by the electrical current flowing through Co-rich microwires that exhibit induced magnetic bistability.

2 Experiment

In order to demonstrate these phenomena, we used amorphous $Co_{69}Fe_4B_{12}Si_{14}C_1$ microwires prepared by using the Taylor–Ulitovky method as described elsewhere [7–11, 14–20]. The studied Co-rich glass-coated microwire presents a diameter of metallic nucleus $d = 25$ μm and a total diameter of $D = 30$ μm. We studied the effect of electrical current on the magnetization switching of as-prepared Co-rich microwires with linear bulk hysteresis loops, and annealed Co-rich microwires with rectangular hysteresis loops. For comparison, we also studied the effect of electrical current on magnetization switching for Fe-rich ($Fe_{75}B_9Si_{12}C_4$) microwires with $d \approx 15.2$ μm and $D \approx 17.2$ μm, and $d \approx 22.1$ μm and $D \approx 24.3$ μm, which exhibit spontaneous magnetic bistability prepared using the same technique.

Prepared $Co_{69}Fe_4B_{12}Si_{14}C_1$ microwire was annealed (at 300°C for 5 min) in order to change the character of the hysteresis loop from a linear one typical of Co-rich as-prepared microwires to a rectangular one typical of annealed Co-rich microwires with low magnetostriction coefficients [19, 20].

For studies of the magnetization switching, we used a Sixtus–Tonks modified setup to evaluate the DW velocity within the microwire. In our experiment, the sample inside the sample holder is placed coaxially inside of the pickup coils. We used three pickup coils (P1, P2, and P3, as shown in Fig. 1) mounted along the length of the wire. If the DW propagates along the sample, it induces an electromotive force (*emf*) in the pickup coils, as described in Refs. [9] and [11].

Each pickup coil is connected to the corresponding input of a digital oscilloscope. Each sharp peak of the *emf* is picked up by an oscilloscope upon passing the propagating wall.

Then, DW velocity is estimated as

$$v = \frac{l}{\Delta t}, \tag{1}$$

where l is the distance between the pickup coils, and Δt is the time difference between the maxima in the induced *emf*.

The difference from previously used setups for studies of magnetic-field-driven DW propagation [16, 17, 27] in magnetic microwires is that instead of a magnetizing solenoid, we used the AC current flowing through the microwire. We used a current amplitude of 10.5 mA, which produced an AC circumferential magnetic field with an amplitude that can be estimated on the surface of the metallic nucleus by using the following formula:

$$H_{circ} = I/(2\pi r), \tag{2}$$

where I is the current value, and r is the radial distance.

From this relation, we estimated that for the $Co_{69}Fe_4B_{12}Si_{14}C_1$ microwire, $H_{circ} \approx 134$ A/m. For

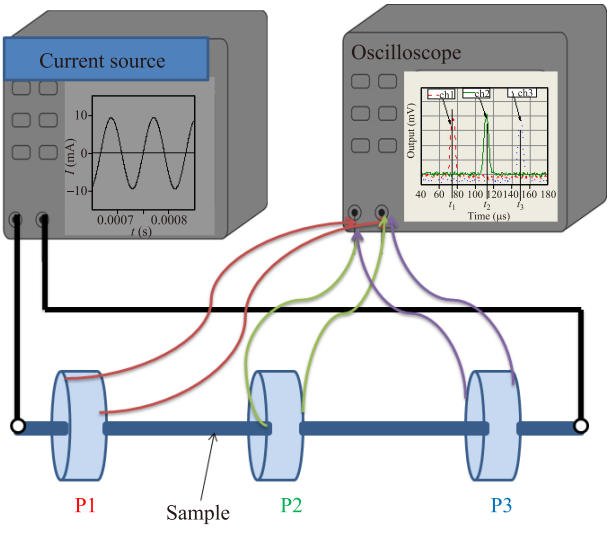

Fig. 1 Schematic of experimental setup.

the $Fe_{75}B_9Si_{12}C_4$ samples ($d \approx 15.2$ and 22.1 μm), $H_{circ} \approx 220$ A/m and 152 A/m, respectively.

For the $Co_{69}Fe_4B_{12}Si_{14}C_1$ sample ($d \approx 25$ μm), the current density j is approximately 21 A/mm^2, while for the $Fe_{75}B_9Si_{12}C_4$ ($d \approx 15.2$ and 22.1 μm) samples, $j \approx 60$ A/mm^2 and 28 A/mm^2, respectively. In all samples, the employed current densities were clearly below the values that can produce magnetic hardening and/or crystallization of the samples [7, 8].

It is worth mentioning that we previously observed the magnetization process induced by electrical current within a thin surface layer using the MOKE method. Using this technique, we were unable to study the inner domain structure and measure domain wall dynamics within the inner part of the sample.

In the present case, we used electrical current and a system of pickup coils previously used for studies of the magnetic-field-driven DW propagation in Fe- and even Co-rich microwires. The experimental setup was completely different from that used in Ref. [26], where the domain wall propagation was induced by an external magnetic field produced by a long solenoid.

We measured the magnetic field dependences of the impedance Z and GMI ratio $\Delta Z/Z$, defined as

$$\Delta Z/Z = [Z(H) - Z(H_{\max})]/Z(H_{\max}), \tag{3}$$

where $H_{\max}$ is the maximum applied DC magnetic field.

We used a specially designed microstrip sample holder. The sample holder was placed inside a sufficiently long solenoid that creates a homogeneous magnetic field H. The sample impedance Z was measured using a vector network analyzer from reflection coefficient S_{11}. A more detailed description of the experimental setup can be found in our previous publications [8, 19, 20].

Hysteresis loops have been measured using a fluxmetric technique described elsewhere [16, 19, 20]. We represent the normalized magnetization M/M_s vs. the magnetic field H, where M is the magnetic moment at a given magnetic field, and M_s is the magnetic moment of the sample at the maximum magnetic field amplitude H_m. The sample length was 10 cm.

Some measurements were performed under tensile stresses. The value of the applied tensile stress within the metallic nucleus and glass shell were calculated as described earlier [28]:

$$\sigma_m = \frac{KP}{KS_m + S_{gl}}, \quad \sigma_{gl} = \frac{P}{KS_m + S_{gl}}, \tag{4}$$

where $K = E_2/E_1$, E_i are the Young's moduli of the metal (E_2) and the glass (E_1) at room temperature, P is the applied mechanical load, and S_m and S_{gl}, respectively, are the cross sections of the metallic nucleus and glass coating.

3 Results and discussion

As-prepared Co-rich microwire presents a linear hysteresis loop with very low remanent magnetization ($Mr/Ms \approx 0.01$) and coercivity $H_c \approx 5$ A/m [Fig. 2(a)]. It is worth mentioning that most experimental results for the amorphous wires were satisfactory explained considering a so-called core-shell model [11–13, 29]. In the case of a Co-rich wire with a negative magnetostriction constant, it is assumed that there is an inner core magnetized along the wire axis and an outer shell where magnetization points in the circumferential direction. Consequently, the linear (almost non-hysteretic) hysteresis loop observed for as-prepared Co-rich microwire must be related to the quasi-reversible magnetization rotation from the circumferential to the axial direction in the outer domain shall with a circumferential easy magnetization direction [13, 29]. Low remanent magnetization must be attributed to the quite small radius of the inner axially magnetized core R_c that can be estimated from remanent magnetization Mr/Ms as [29]

$$R_c = R(Mr/Ms)^{1/2}, \tag{5}$$

where R is the wire radius. Considering the low Mr/Ms values ($Mr/Ms \approx 0.01$) obtained from Fig. 2(a), we estimate that R_c is approximately $0.1R$, meaning that the inner core volume in the as-prepared sample is quite low.

An annealed Co-rich sample and as-prepared Fe-rich samples present a perfectly rectangular hysteresis loop shape that reflects the fast magnetization switching of the studied sample [Figs. 2(b), (c)]. Considering relation (5), we can estimate that $R_c \approx 0.9R$ and $R_c \approx 0.97R$ for the annealed Co-rich sample and Fe-rich sample, respectively. Consequently, after the annealing of Co-rich microwires, we observed that the inner axially magnetized core volume and coercivity increased.

As discussed elsewhere [9–12, 23, 30], the rectangular character of a hysteresis loop characterized by a single and large Barkhausen jump is related to the domain structure of the magnetic wires [23, 24]. It is commonly assumed and confirmed by direct and indirect measurements that the domain structure of amorphous microwires exhibiting rectangular hysteresis loops consists of a single large axially magnetized domain and an external domain structure with transversal magnetization at the surface [11–13]. A radially magnetized outer domain is considered in the case of Fe-rich microwires, while a circumferential magnetization orientation is proposed for Co-rich microwires [11–13].

The annealed Co-rich sample and Fe-rich samples present quite similar hysteresis loops with coercivities of approximately 45 A/m. The most appreciated difference is that the Co-rich microwire presents a higher magnetic

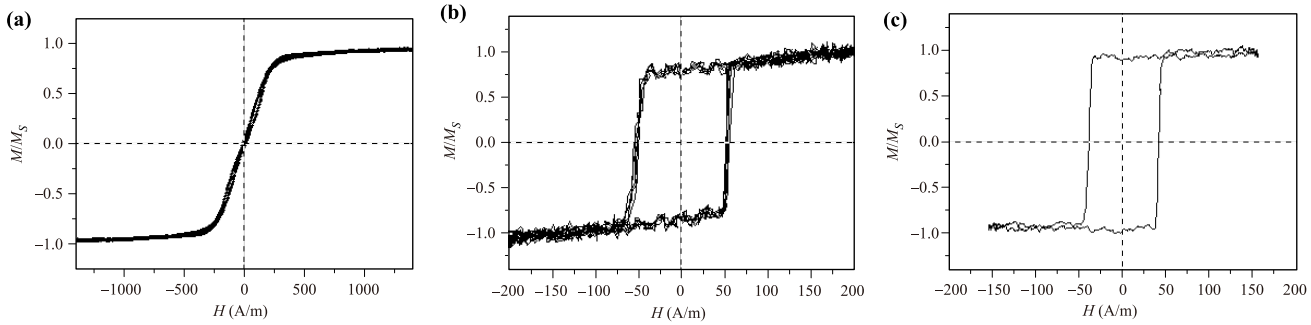

Fig. 2 Hysteresis loops of **(a)** as-prepared $Co_{69}Fe_4B_{12}Si_{14}C_1$ microwire, **(b)** annealed at 300°C for 5 min $Co_{69}Fe_4B_{12}Si_{14}C_1$ microwire, and **(c)** as-prepared $Fe_{75}B_9Si_{12}C_4$ microwire.

permeability in the remanent state, which is reflected by a higher slope of the flat regions of the hysteresis loops (see Fig. 2). Therefore, the outer domain structure of the annealed Co-rich sample can be different from that of the Fe-rich sample.

We measured $\Delta Z/Z(H)$ dependences for as-prepared $Fe_{75}B_9Si_{12}C_4$ (presenting spontaneous magnetic bistability) and as-prepared (with a linear hysteresis loop) and annealed $Co_{69}Fe_4B_{12}Si_{14}C_1$ (presenting induced magnetic bistability) samples with the frequency as a parameter [see Figs. 3(a)–(c)]. As can be observed, there is a considerable difference in the $\Delta Z/Z(H)$ dependences and in the value of the maximum GMI ratio $\Delta Z/Z_{max}$. First, the $Fe_{75}B_9Si_{12}C_4$ microwire has a $\Delta Z/Z_{max}$ value that is almost one order lower than that of the as-prepared and annealed $Co_{69}Fe_4B_{12}Si_{14}C_1$ samples (18%, 270%, and 170%, respectively). Second, the $\Delta Z/Z(H)$ dependence measured for the $Fe_{75}B_9Si_{12}C_4$ sample exhibits decay from $\Delta Z/Z(H = 0)$, while the as-prepared and annealed $Co_{69}Fe_4B_{12}Si_{14}C_1$ microwires exhibit double maximum $\Delta Z/Z(H)$ dependences. Such $\Delta Z/Z(H)$ dependence double maximum is usually associated with circumferential magnetic anisotropy, while the $\Delta Z/Z(H)$ exhibiting a decay (as we observed in the Fe-rich sample) is usually associated with longitudinal magnetic anisotropy [22, 23, 31].

Consequently, from measurements of the hysteresis loops and the GMI effect, we can i) assume the existence of the inner axially magnetized domain responsible for the magnetically bistable behavior in the annealed Co-rich sample and Fe-rich sample, but also ii) different magnetic anisotropy in the outer domain shell for Co-rich and Fe-rich microwires with spontaneous and induced magnetic bistability. It is worth mentioning that the circumferential magnetization anisotropy in the Co-rich sample with induced magnetic bistability was recently confirmed by MOKE [26].

As mentioned in the introduction, recently we observed the magnetostatic interaction of the inner axially magnetized core and the outer domain shell that caused a GMI hysteresis [25].

In our experiment, we applied an AC electrical current producing a circumferential AC magnetic field that must affect the magnetization of the outer shell with a circumferentially magnetization easy axis.

In Figs. 4(a)–(c), the electromotive force (EMF) signals ε, generated in the pickup coils by the magnetization changes caused by the current in all studied samples, are

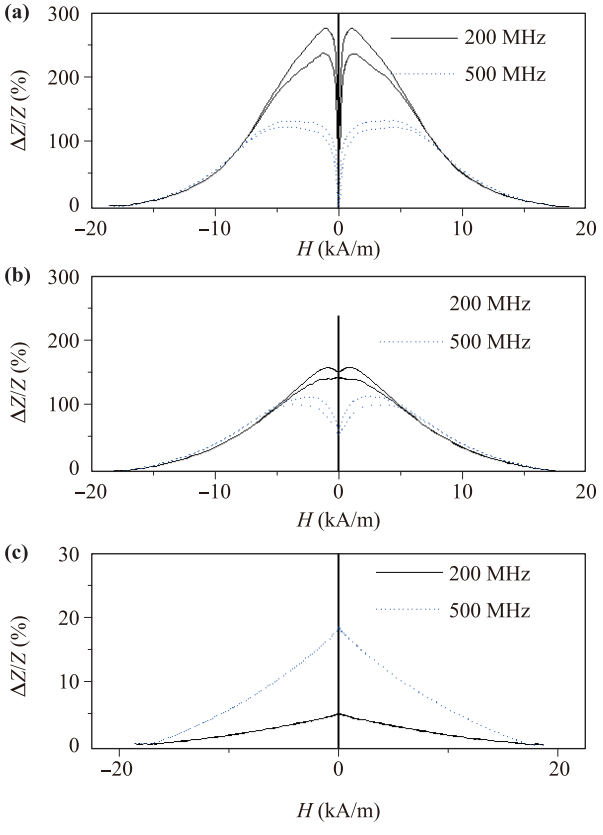

Fig. 3 $\Delta Z/Z(H)$ dependences measured in **(a)** as-prepared and **(b)** annealed at $T_{ann} = 300°C$ for $t_{ann} = 5$ min $Co_{69}Fe_4B_{12}Si_{14}C_1$ microwire, and **(c)** in as-prepared $Fe_{75}B_9Si_{12}C_4$ microwire measured at different frequencies.

shown. As can be observed, appreciable EMF peaks with quite similar amplitudes were induced in the pickup coils for the annealed $Co_{69}Fe_4B_{12}Si_{14}C_1$ sample, while for the as-prepared $Fe_{75}B_9Si_{12}C_4$, the EMF voltages induced in all pickup coils was quite small [Fig. 4(b)]. For comparison, we measured time t and the dependence of the EMF signals ε for $Fe_{75}B_9Si_{12}C_4$ with a thicker metallic nucleus diameter ($d \approx 22.1$ μm), and a similar glass-coating thickness (approximately 1.1 μm), which is provided in the inset of Fig. 4(b). A thicker $Fe_{75}B_9Si_{12}C_4$ microwire also presents rather low EMF voltages induced in all pickup coils.

Additionally, small systematic temporal shifts on the t-axis between the EMF peaks can be observed for the annealed $Co_{69}Fe_4B_{12}Si_{14}C_1$ sample [Fig. 4(a)].

In the as-prepared $Co_{69}Fe_4B_{12}Si_{14}C_1$ sample (with a linear hysteresis loop), similar to the annealed $Co_{69}Fe_4B_{12}Si_{14}C_1$ sample, we observed appreciable EMF peaks. However, in contrast to the annealed sample, we did not observe a temporal shift that could be appreciated on the t-axis for the annealed $Co_{69}Fe_4B_{12}Si_{14}C_1$ sample [Fig. 4(c)].

To interpret the observed dependences, we must consider different the domain structures of the studied samples. As discussed above, a linear hysteresis loop with vanishing remanent magnetization observed in an as-prepared Co-rich microwire must be related to the magnetization rotation process.

The other two samples (annealed Co-rich sample and as-prepared Fe-rich sample) present perfectly rectangular hysteresis loops usually related to the inner axially magnetized single-domain core [12, 13].

Consequently, the smallest EMF signals observed in Fe-rich microwires can be explained considering that the circular magnetic field produced by electrical current does not sufficiently affect the radially magnetized outer domain typically observed in Fe-rich microwires [12].

The amplitudes of the EMF peaks induced in the pickup coil of the annealed sample are quite similar to those observed in the as-prepared sample [Figs. 4(a), (c)].

As previously discussed, a bamboo-like domain structure is typically observed in the outer shell of Co-rich magnetic wires with low and negative magnetostriction [11–13]. Consequently, we can assume that appreciable EMF peaks induced in the pickup coils can be attributed to the magnetization changes in the outer domain shell induced by the circular magnetic field produced by electrical current (Oersted field). EMF peaks observed in as-prepared $Co_{69}Fe_4B_{12}Si_{14}C_1$ microwires, in our opinion, mean that the electrical current affects the outer bamboo-like domain shell with a circular magnetization orientation.

On the other hand, considering the low Mr/Ms-values (as mentioned above) observed in Fig. 2(a), we determined that the inner core volume of as-prepared $Co_{69}Fe_4B_{12}Si_{14}C_1$ sample is quite low, and the main part of the sample presents a circumferential magnetization orientation, i.e., the outer domain shell of as-prepared Co-rich microwire is much thicker. Aforementioned considerations of the domain structure [made considering

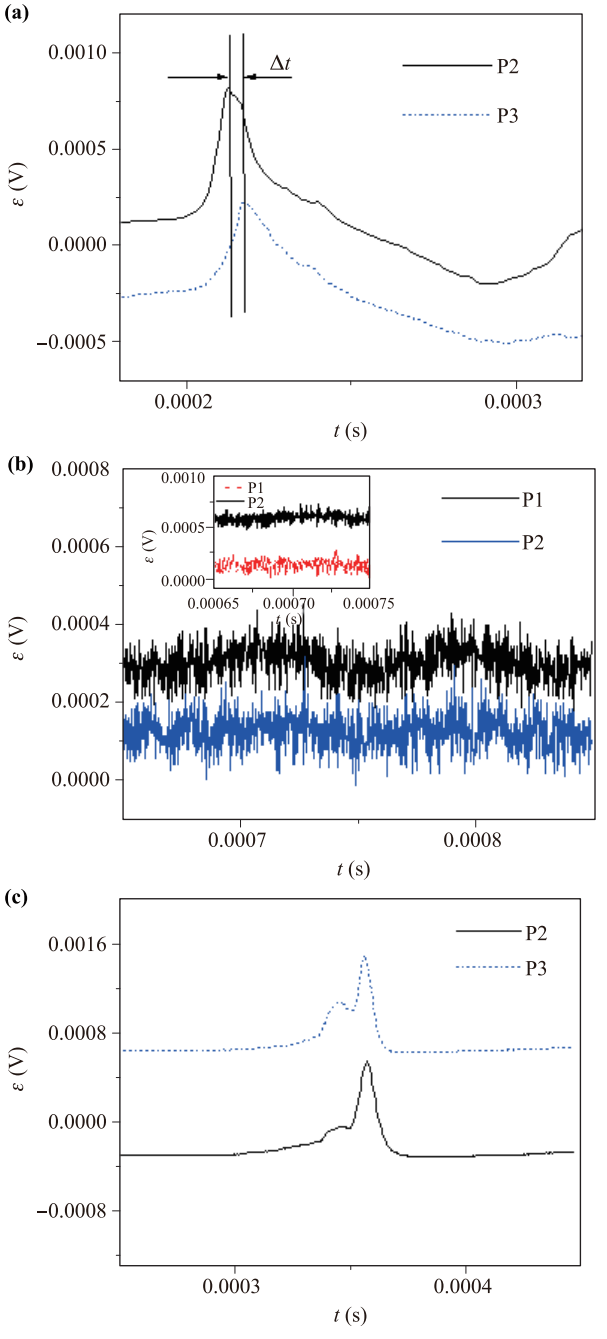

Fig. 4 Voltage peaks induced by magnetization changes in pickup coils in **(a)** annealed $Co_{69}Fe_4B_{12}Si_{14}C_1$, **(b)** as-prepared $Fe_{75}B_9Si_{12}C_4$, and **(c)** $Co_{69}Fe_4B_{12}Si_{14}C_1$ microwires.

different $\Delta Z/Z(H)$ dependences and different characters of hysteresis loops with rather different Mr/Ms values)] of all studied samples are schematically summarized in Fig. 5.

Consequently, we consider that the magnetization process of the inner axially magnetized core in annealed $Co_{69}Fe_4B_{12}Si_{14}C_1$ microwire contributes to the induced EMF peaks in the pickup coils.

The difference in the EMF signals of the as-prepared and annealed $Co_{69}Fe_4B_{12}Si_{14}C_1$ samples is that we observed a systematic temporal shift Δt between the EMF peaks for the annealed $Co_{69}Fe_4B_{12}Si_{14}C_1$ sample [Fig. 6(a)]. This shift is not observed for the as-prepared $Co_{69}Fe_4B_{12}Si_{14}C_1$ sample [Fig. 6(c)]. This shift becomes even more visible under tensile stress applied during the measurements of the annealed $Co_{69}Fe_4B_{12}Si_{14}C_1$ sample [Fig. 6(b)].

Additionally, we observed a significant increase in the amplitude of the EMF peaks in the annealed $Co_{69}Fe_4B_{12}Si_{14}C_1$ sample measured under tensile stress [appreciable from a comparison of Figs. 6(a) and 6(b)]. However, the amplitude of the EMF peaks for the as-prepared $Co_{69}Fe_4B_{12}Si_{14}C_1$ sample measured under stress remained unchanged [Fig. 6(c)].

We can explain our observed differences by considering the different magnetization processes of the as-prepared and annealed $Co_{69}Fe_4B_{12}Si_{14}C_1$ samples.

We consider that the temporal shift between the peaks in the annealed $Co_{69}Fe_4B_{12}Si_{14}C_1$ sample is related to the magnetization switching in the inner core by domain wall propagation along the microwire. Moreover, from the shift between the peaks, we can estimate the velocity of the propagating domain wall from (1). Using this method, we obtained a DW velocity of approximately 4.5 km/s, i.e., values quite similar to those reported in Co-rich microwires with induced magnetic bistability [19, 20].

From the observed dependence of the temporal shift Δt on the applied stress σ, we can estimate the dependence of DW velocity on tensile stress (see Fig. 7).

The observed DW propagation along the sample induced by the current flowing through the microwire was explained by considering the magnetostatic interaction between the outer circumferentially magnetized shall and the inner axially magnetized core. Indeed, the Oersted magnetic field produced by the current is largest on the surface, and therefore must affect mostly the outer domain shell with a circumferential magnetization orientation. However, we recently observed the magnetostatic interaction of the inner axially magnetized core with the outer domain shell [23]. Therefore, we expect that magnetization switching induced in the outer domain shell

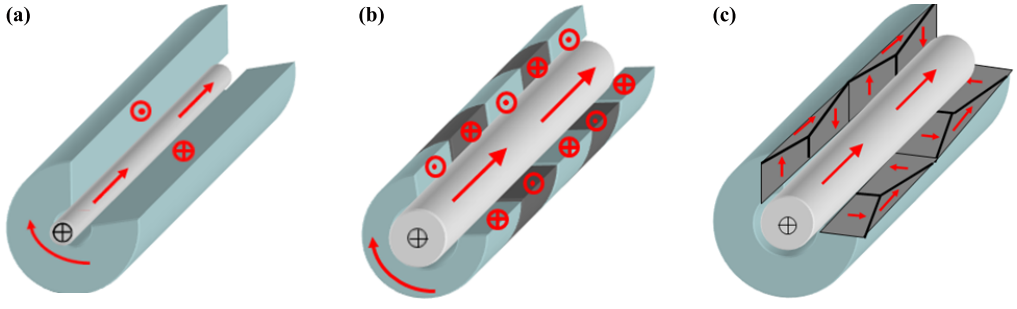

Fig. 5 Schematic domain structure of **(a)** as-prepared, **(b)** annealed at 300°C for 5 min, and **(c)** $Co_{69}Fe_4B_{12}Si_{14}C_1$ amorphous microwire and $Fe_{75}B_9Si_{12}C_4$ microwire.

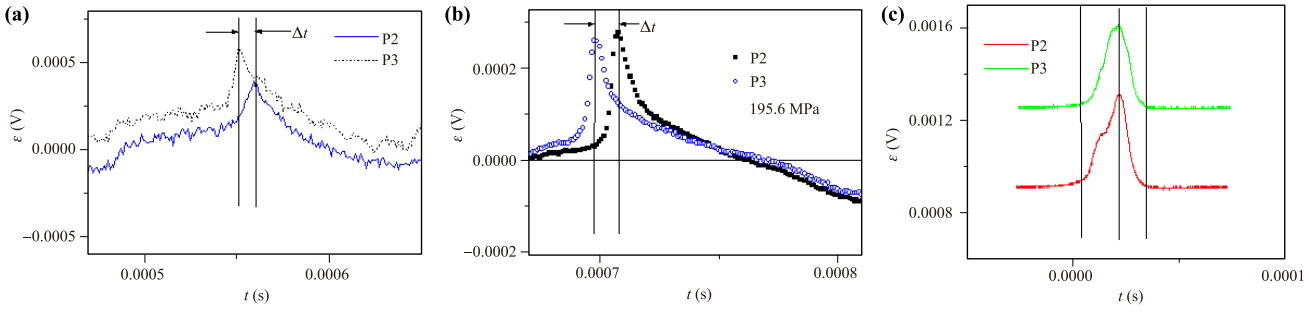

Fig. 6 EMF peaks induced by magnetization changes in pickup coils measured in annealed $Co_{69}Fe_4B_{12}Si_{14}C_1$ sample: **(a)** without stress, **(b)** under tensile stress of 195.6 MPa, and **(c)** in as-prepared $Co_{69}Fe_4B_{12}Si_{14}C_1$ sample under tensile stress of 195.6 MPa.

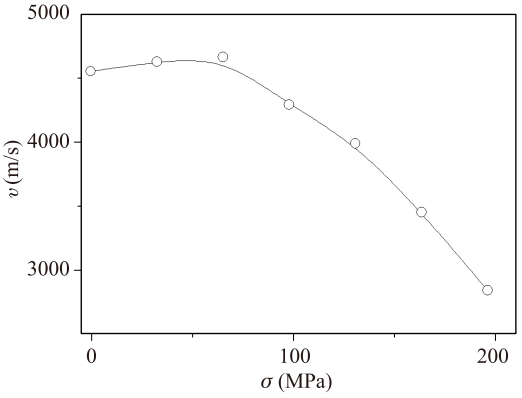

Fig. 7 Dependence of DW velocity on applied tensile stress estimated for annealed $Co_{69}Fe_4B_{12}Si_{14}C_1$ microwire.

by electric current can affect the magnetization in the inner core.

With regard to the effect of applied tensile stresses on the amplitude of the EMF peaks observed in the annealed $Co_{69}Fe_4B_{12}Si_{14}C_1$ sample, we must consider the influence of the stresses on domain wall propagation.

The EMF generated within the turn of the pickup coil by a change in the magnetic flux is given by

$$\varepsilon(t) = -\frac{4\pi}{c}\frac{\partial \Phi}{\partial t}, \tag{6}$$

where c is the velocity of light, $\Phi = BS$ is the magnetic flux, S is the area of the surface, $B = M + H$ is the magnetic induction, and M is the magnetization. Thus, the amplitude of the EMF peaks must be determined by $\frac{\partial M}{\partial t}$.

The EMF signals generated by a head-to-head DW moving through the magnetic wire are studied in Ref. [32]. In particular, it was found that the characteristic width δ of a head-to-head DW is determined by the magnetoelastic anisotropy. The reduced head-to-head domain wall width δ/d (d is the metallic nucleus diameter) depends on the value of the anisotropy constant K. It is determined that $\delta/d \approx 13.5$ for $K = 10^4$ erg/cm^3, $\delta/d \approx 20$ for $K = 5 \times 10^3$ erg/cm^3, $\delta/d = 30 - 34$ for $K = 2 \times 10^3$ erg/cm^3, and $\delta/d = 40 - 50$ for $K = 103$ erg/cm^3. Moreover, decreasing δ/d with an increase in the internal stresses (determined by the ratio of metallic nucleus diameter d to the total microwire diameter D) is reported.

Similar conclusions on the stress dependence of the DW shape and DW width were made for different families of magnetic wires [33–35] and thin films [36].

A decrease in the characteristic width δ must be associated with $\frac{\partial M}{\partial t}$ increasing, as schematically shown in Fig. 8.

On the other hand, the observed dependence of the velocity of DW propagation on the tensile stress (see Fig. 7) must be explained considering that the domain wall mobility S is proportional to the domain wall width δ [16]:

$$S \sim \delta \sim (A/K)^{1/2}, \tag{7}$$

where A is the exchange stiffness constant, and K is the magnetic anisotropy constant.

In amorphous materials, the main source of magnetic anisotropy is the magnetoelastic anisotropy K_{me}, which is given by

$$K_{me} \approx 3/(2\lambda_s \sigma), \tag{8}$$

where σ is the stress, and λ_s is the magnetostriction coefficient.

For magnetic-field-driven DW dynamics (viscous regime), the DW velocity is proportional to the DW mobility according to the expression

$$v = S(H - H_0), \tag{9}$$

where H is the axial magnetic field, and H_0 is the critical propagation field, below which domain wall propagation is not possible.

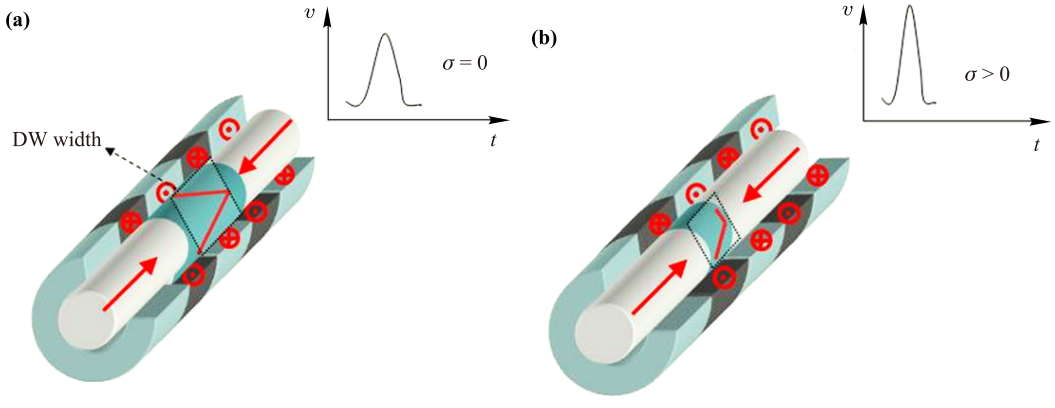

Fig. 8 Schematic pictures of DW and EMF signal in $Co_{69}Fe_4B_{12}Si_{14}C_1$ **(a)** without stress and **(b)** with stress.

Consequently, we can expect a reduction in the DW velocity under applied stress.

With regard to the stress dependence of the EMF signals, it is worth noting that when previously using the MOKE method, we observed that the circular magnetic bistability (i.e., the rectangular hysteresis loop of the transversal magnetization vs. the electrical current) could be induced by the tensile stress. Such circular magnetic bistability has been explained considering the transformation of the circular multidomain bamboo-like structure observed in the absence of tensile stress into a single-domain structure [10]. These changes were previously observed using MOKE [10, 37], and were attributed to the stress-induced changes in the energy of the magnetic system associated with the enhancement of the magneto-elastic anisotropy, and therefore the enhancement of the domain wall energy.

The observed enhancement of the signals in the pickup coils under applied stress can be also attributed to the aforementioned changes in the surface domain structure from the multidomain bamboo-like structure into a single-domain one.

It is worth mentioning that the enhancement of the amplitude of the EMF peaks under tensile stress is observed only for the annealed $Co_{69}Fe_4B_{12}Si_{14}C_1$ sample [Fig. 6(b)]. The amplitude of the EMF peaks of the as-prepared $Co_{69}Fe_4B_{12}Si_{14}C_1$ sample (presenting a linear hysteresis loop) is not affected by the tensile stress [Fig. 6(c)].

Considering the aforementioned discussion, we can assume that the outer circular domain structure of the as-prepared $Co_{69}Fe_4B_{12}Si_{14}C_1$ sample is instead a single domain [as shown in Fig. 5(a)], as it was experimentally and theoretically reported elsewhere [38, 39].

In fact, it was theoretically predicted elsewhere [38, 39] that a single stable cylindrical domain can be created in an amorphous Co-rich microwire. On the other hand, the circular magnetic bistability reportedly induced by tensile stress in some glass-covered Co-rich microwires [10] is related to the single-domain structure of the outer domain shell of Co-rich microwires.

The assumed transformation of a single-domain structure into a bamboo-like-domain cylindrical structure of the outer shell of Co-rich magnetic microwires after annealing might be related to internal stress relaxation. Indeed, the internal stresses arising during the preparation of glass-coated microwires originate from three different phenomena: i) stresses associated with the rapid solidification from the melt, ii) different thermal expansion coefficients of quenching the metallic ingot and glass coating, and iii) tensile drawing stresses [40, 41]. From the radial distribution of the total internal stresses reported elsewhere [40, 41], one can see that the tensile internal stresses are strongest within the main part of the metallic nucleus [40, 41]. Consequently, annealing that allows for internal stress relaxation must be considered as a release of tensile stresses. Hence, one can expect diminishing of the magneto-elastic anisotropy, and therefore diminishing of the domain wall energy and transformation of a single-domain structure into a bamboo-like structure.

With regard to the origin of the observed DW propagation induced by the current flowing through the annealed Co-rich microwire, we considered the magnetostatic interaction between the outer circumferentially magnetized shell and the inner axially magnetized core. We assume that flowing current produces a circumferential magnetic field that affects the magnetization of the outer shell.

As discussed elsewhere [11, 39, 42], the magnetization distribution inside the magnetic wires is determined by the total energy of the wire, which consists of exchange, magnetoelastic, and Zeeman energy contributions. Therefore, we must assume that if the magnetization of the outer domain shell changes (i.e., under a circular field produced by the current), this can affect the overall magnetization distribution within the wire. Indeed, for the $Co_{69}Fe_4B_{12}Si_{14}C_1$ sample, AC current produces $H_{circ} \approx 134$ A/m. For the $Fe_{75}B_9Si_{12}C_4$ sample, $H_{circ} \approx 220$ A/m. However, as we observed above, this sample does not present DW propagation under AC current. This difference can be explained by considering the different magnetization easy directions in annealed Co-rich and Fe-rich microwires. For the circumferentially oriented outer domain shell typical of Co-rich wire, the current can produce a remagnetization of the outer circularly magnetized shell if the current amplitude is high enough. Consequently, remagnetization of the outer shell affects the magnetization in the inner core through the magnetostatic interaction between them. For the radially magnetized outer domain shell typical of Fe-rich wires, the current likely produces a magnetization rotation that does not affect the magnetization in the inner axially magnetized core.

It is worth mentioning that the magnetostatic interaction of the inner axially magnetized core and the outer domain shell has been demonstrated experimentally (by the shift in the MI curve along the axial magnetic field), by a shift of the circular hysteresis loop under application of an axial magnetic field, and from the dependence of the remanent circular magnetization component measured and calculated for various inner-core diameters [25, 37].

Consequently, the domain structure realized in annealed Co-rich microwire with an induced magnetic bistability consisting of an inner axially magnetized core and outer shell with a circumferential easy magnetization direction is essentially favorable for observing single-domain wall propagation induced by electrical current.

4 Conclusions

Under certain experimental conditions, we realized the remagnetization of annealed Co-rich microwire by fast domain wall propagation along the microwire under the influence of the AC current flowing through the sample.

The estimated DW velocity is approximately 4.5 km/s. This is similar to and even higher than that reported for the magnetic-field-driven domain wall propagation in Fe- and Co-rich microwires.

We discussed different magnetization reversals of all studied microwires considering a comparison of hysteresis loops, the GMI effect, and the stress dependence of the EMF generated in the pickup coils.

The observed DW propagation induced by the current flowing through the microwire was discussed considering the influence of an Oersted magnetic field produced by electrical current on the outer domain shell. This field had a circular magnetization orientation and magnetostatic interaction between the outer circumferentially magnetized shell and the inner axially magnetized core.

Acknowledgements This work was supported by Spanish MINECO under MAT2013-47231-C2-1-P, by the Basque Government under an Elkartek RTM 4.0 grant, and under the scheme of "Ayuda a Grupos Consolidados" (Ref. IT954-16) and the National Science Centre Doland under grant DEC-2016/22/M/ST3/00471. Technical and human support was provided by SGIker (UPV/EHU) and is gratefully acknowledged. A. Chizhik and V. Zhukova wish to acknowledge the support of the Basque Government under the Program of Mobility of the Investigating Personnel of the Department of Education, Universities and Investigation (grants MV-2017-1-0025, MV-2017-1-0003, and MV-2017-1-0030).

References

1. T. Ono, H. Miyajima, K. Mibu, N. Hosoito, and T. Shinjo, Propagation of a magnetic domain wall in a submicrometer magnetic wire, *Science* 284(5413), 468 (1999)
2. D. A. Allwood, G. Xiong, C. C. Faulkner, D. Atkinson, D. Petit, and R. P. Cowburn, Magnetic domain-wall logic, *Science* 309(5741), 1688 (2005)
3. K. J. Sixtus and L. Tonks, Propagation of large Barkhausen discontinuities (II), *Phys. Rev.* 42(3), 419 (1932)
4. A. P. Malozemoff and J. C. Slonczewski, Magnetic Domain Walls in Bubble Materials, New York: Academic Press, 1979
5. A. Kunz, Field induced domain wall collisions in thin magnetic nanowires, *Appl. Phys. Lett.* 94(13), 132502 (2009)
6. M. Hayashi, L. Thomas, Ch. Rettner, R. Moriya, X. Jiang, and S. Parkin, Dependence of current and field driven depinning of domain walls on their structure and chirality in permalloy nanowires, *Phys. Rev. Lett.* 97(20), 207205 (2006)
7. V. Zhukova, A. F. Cobeño, A. Zhukov, J. M. Blanco, S. Puerta, J. Gonzalez, and M. Vázquez, Tailoring of magnetic properties of glass-coated microwires by current annealing, *J. Non-Cryst. Solids* 287(1–3), 31 (2001)
8. V. Zhukova, M. Ipatov, J. González, J. M. Blanco and A. P. Zhukov, Development of thin microwires with enhanced magnetic softness and GMI, *IEEE Trans. Magn.* 44(Part 2), 3958 (2008)
9. A. Vanhaverbeke, A. Bischof, and R. Allenspach, Control of domain wall polarity by current pulses, *Phys. Rev. Lett.* 101(10), 107202 (2008)
10. J. Gonzalez, A. Chizhik, A. Zhukov, and J. M. Blanco, Surface magnetization reversal and magnetic domain structure in amorphous microwires, *Phys. Status Solidi. A* 208(3), 502 (2011)
11. V. Zhukova, N. A. Usov, A. Zhukov, and J. Gonzalez, Length effect in a Co-rich amorphous wire, *Phys. Rev. B* 65(13), 134407 (2002)
12. Yu. Kabanov, A. Zhukov, V. Zhukova, and J. Gonzalez, Magnetic domain structure of wires studied by using the magneto-optical indicator film method, *Appl. Phys. Lett.* 87(14), 142507 (2005)
13. J. N. Nderu, M. Takajo, J. Yamasaki, and F. B. Humphrey, Effect of stress on the bamboo domains and magnetization process of CoSiB amorphous wire, *IEEE Trans. Magn.* 34(4), 1312 (1998)
14. A. Zhukov, J. M. Blanco, A. Chizhik, M. Ipatov, V. Rodionova, and V. Zhukova, Manipulation of domain wall dynamics in amorphous microwires through domain wall collision, *J. Appl. Phys.* 114(4), 043910 (2013)
15. H. Chiriac, T. A. Ovari, and M. Tibu, Domain wall propagation in nearly zero magnetostrictive amorphous microwires, *IEEE Trans. Magn.* 44(11), 3931 (2008)
16. V. Zhukova, J. M. Blanco, V. Rodionova, M. Ipatov, and A. Zhukov, Domain wall propagation in micrometric wires: Limits of single domain wall regime, J. Appl. Phys. 111, 07E311 (2012)
17. M. Vázquez, G. A. Basheed, G. Infante, and R. P. Del Real, Trapping and injecting single domain walls in magnetic wire by local fields, *Phys. Rev. Lett.* 108(3), 037201 (2012)
18. R. Gemperle, L. Kraus, and J. Schneider, Magnetization reversal in amorphous $(Fe_{1-x}Ni_x)_{80}P_{10}B_{10}$microwires, J. Phys. B 28(10), 1138 (1978)
19. A. Zhukov, A. Talaat, M. Ipatov, J. M. Blanco, and V. Zhukova, Tailoring of magnetic properties and GMI effect of Co-rich amorphous microwires by heat treatment, *J. Alloys Compd.* 615, 610 (2014)

20. A. Talaat, M. Churyukanova, J. M. Blanco, M. Ipatov, V. Zhukova, and A. Zhukov, Simultaneous detection of giant magnetoimpedance and fast domain wall propagation in Co-based glass-coated microwires, *IEEE Magn. Lett.* 7, 5200604 (2016)
21. M. H. Phan and H. X. Peng, Giant magnetoimpedance materials: Fundamentals and applications, *Prog. Mater. Sci.* 53(2), 323 (2008)
22. L. V. Panina and K. Mohri, Magneto-impedance effect in amorphous wires, *Appl. Phys. Lett.* 65(9), 1189 (1994)
23. A. Zhukov, M. Ipatov, and V. Zhukova, Advances in giant magnetoimpedance of materials, *Handbook of Magnetic Materials*, ed. K. H. J. Buschow, 24: Chapter 2, 139–236, 2015
24. T. Uchiyama, K. Mohri, and Sh. Nakayama, Measurement of spontaneous oscillatory magnetic field of guinea-pig smooth muscle preparation using pico-Tesla resolution amorphous wire magneto-impedance sensor, *IEEE Trans. Magn.* 47(10), 3070 (2011)
25. M. Ipatov, V. Zhukova, J. Gonzalez, and A. Zhukov, Magnetoimpedance hysteresis in amorphous microwires induced by core–shell interaction, *Appl. Phys. Lett.* 105(12), 122401 (2014)
26. A. Zhukov, A. Chizhik, M. Ipatov, A. Talaat, J. M. Blanco, A. Stupakiewicz, and V. Zhukova, Giant magnetoimpedance effect and domain wall dynamics in Co-rich amorphous microwires, *J. Appl. Phys.* 117(4), 043904 (2015)
27. R. Varga, A. Zhukov, J. M. Blanco, M. Ipatov, V. Zhukova, J. Gonzalez, and P. Vojtaník, Fast magnetic domain wall in magnetic microwires, *Phys. Rev. B* 74(21), 212405 (2006)
28. A. Zhukov, Design of the magnetic properties of Fe-rich, glass-coated microwires for technical applications, *Adv. Funct. Mater.* 16(5), 675 (2006)
29. M. Vázquez and D. X. Chen, The magnetization reversal process in amorphous wires, *IEEE Trans. Magn.* 31(2), 1229 (1995)
30. A. Zhukov, Domain wall propagation in a Fe-rich glass-coated amorphous microwire, *Appl. Phys. Lett.* 78(20), 3106 (2001)
31. N. A. Usov, A. S. Antonov, and A. N. Lagar'kov, Theory of giant magneto-impedance effect in amorphous wires with different types of magnetic anisotropy, *J. Magn. Magn. Mater.* 185(2), 159 (1998)
32. S. A. Gudoshnikov, Yu. B. Grebenshchikov, B. Ya. Ljubimov, P. S. Palvanov, N. A. Usov, M. Ipatov, A. Zhukov, and J. Gonzalez, Ground state magnetization distribution and characteristic width of head to head domain wall in Fe-rich amorphous microwire, *Phys. Status Solidi. A* 206(4), 613 (2009)
33. L. V. Panina, M. Mizutani, K. Mohri, F. R. Humphrey, and L. Ogasawara, Dynamics and relaxation of large Barkhausen discontinuity in amorphous wires, *IEEE Trans. Magn.* 27(6), 5331 (1991)
34. L. V. Panina, M. Ipatov, V. Zhukova, and A. Zhukov, Domain wall propagation in Fe-rich amorphous microwires, *Physica B* 407(9), 1442 (2012)
35. D. X. Chen, N. M. Dempsey, M. Vázquez, and A. Hernando, Propagating domain wall shape and dynamics in iron-rich amorphous wires, *IEEE Trans. Magn.* 31(1), 781 (1995)
36. P. M. Shepley, A. W. Rushforth, M. Wang, G. Burnell, and T. A. Moore, Modification of perpendicular magnetic anisotropy and domain wall velocity in Pt/Co/Pt by voltage-induced strain, *Sci. Rep.* 5(1), 7921 (2015)
37. A. Chizhik, V. Zablotskii, A. Stupakiewicz, C. Gómez-Polo, A. Maziewski, A. Zhukov, J. Gonzalez, and J. M. Blanco, Magnetization switching in ferromagnetic microwires, *Phys. Rev. B* 82(21), 212401 (2010)
38. N. A. Usov and S. A. Gudoshnikov, Circular magnetization process in amorphous microwire with negative magnetostriction, *J. Phys. D* 49(16), 165001 (2016)
39. N. Usov, A. Antonov, A. Dykhne, and A. Lagar'kov, Possible origin for the bamboo domain structure in Co-rich amorphous wire, *J. Magn. Magn. Mater.* 174(1–2), 127 (1997)
40. A. S. Antonov, V. T. Borisov, O. V. Borisov, A. F. Prokoshin, and N. A. Usov, Residual quenching stresses in glass-coated amorphous ferromagnetic microwires, *J. Phys. D* 33(10), 1161 (2000)
41. H. Chiriac, T. A. Óvári, and A. Zhukov, Magnetoelastic anisotropy of amorphous microwireS, *J. Magn. Magn. Mater.* 254–255, 469 (2003)
42. M. Ipatov, V. Zhukova, A. Zhukov, J. Gonzalez, and A. Zvezdin, Low-field hysteresis in the magnetoimpedance of amorphous microwires, *Phys. Rev. B* 81(13), 134421 (2010)